

Hemilabile Properties of the η^3 -Diphenylvinylphosphine (DPVP) Phosphaallyl Ligand: Synthesis and Reactions of $[(\eta^5\text{-C}_5\text{Me}_5)\text{Ru}(\eta^3\text{-DPVP})(\eta^1\text{-DPVP})]\text{PF}_6$

Luis P. Barthel-Rosa,[†] Kalyani Maitra,[†] Jean Fischer,[‡] and John H. Nelson^{*,†}

Department of Chemistry/216, University of Nevada—Reno, Reno, Nevada 89557-0020,
and Laboratoire de Cristallochimie (URA 424 du CNRS), Université Louis Pasteur,
4 rue Blaise Pascal, F-67070 Strasbourg Cedex, France

Received December 17, 1996[®]

Pentamethylcyclopentadienyl-ruthenium(II) half-sandwich complexes containing the olefinic phosphine ligand diphenylvinylphosphine (DPVP) are described. The hemilabile properties of the η^3 -DPVP ligand, a neutral monometallic phosphaallyl, are illustrated by reactions with carbon monoxide and terminal acetylenes. DPVP reacts with $[(\eta^5\text{-C}_5\text{Me}_5)\text{RuCl}_2]_2$ to give the disubstituted ruthenium(II) compound $[(\eta^5\text{-C}_5\text{Me}_5)\text{Ru}(\eta^3\text{-DPVP})(\eta^1\text{-DPVP})]\text{PF}_6$ (**1**). **1** reacts with NaNCS to form $[(\eta^5\text{-C}_5\text{Me}_5)\text{Ru}(\eta^1\text{-DPVP})_2(\text{NCS})]\text{PF}_6$ (**2**). **1** reacts with CO, $\text{HC}\equiv\text{CPh}$, $\text{HC}\equiv\text{CCH}_2\text{CH}_2\text{OH}$, and $\text{HC}\equiv\text{CCH}_2\text{OH}$ to form $[(\eta^5\text{-C}_5\text{Me}_5)\text{Ru}(\eta^1\text{-DPVP})_2(\text{CO})]\text{PF}_6$ (**3**), $[(\eta^5\text{-C}_5\text{Me}_5)\text{Ru}(\eta^1\text{-DPVP})_2\{\text{C}=\text{C}(\text{H})(\text{Ph})\}]\text{PF}_6$ (**4**), $[(\eta^5\text{-C}_5\text{Me}_5)\text{Ru}(\eta^1\text{-DPVP})_2\{\text{C}(\text{CH}_2)_3\text{O}\}]\text{PF}_6$ (**5**), and $[(\eta^5\text{-C}_5\text{Me}_5)\text{Ru}(\eta^1\text{-DPVP})_2\{\text{C}=\text{C}(\text{H})(\text{CH}_2\text{OH})\}]\text{PF}_6$ (**6**), respectively. **6** slowly decomposes in aerated solutions to form **3**, presumably through an allenylidene intermediate. **6** reacts with excess DPVP and HPF_6 to form the novel, *P,P*-diphenyltrihydrophosphonium vinylidene compound $[(\eta^5\text{-C}_5\text{Me}_5)\text{Ru}(\eta^1\text{-DPVP})_2\{\text{C}=\text{C}(\text{CH}_2)_2\text{PPh}_2\text{CH}_2\}]\text{PF}_6$ (**7**). The characteristic ^1H , $^{13}\text{C}\{^1\text{H}\}$, and $^{31}\text{P}\{^1\text{H}\}$ spectroscopic features of all compounds are described. The molecular structures of compounds **1**, **4**, **5**, and **7** have been determined by single crystal X-ray crystallography.

Introduction

One of many expanding areas of interest in organometallic chemistry is the use of "hybrid" ligands¹ on transition metal complexes. Hybrid ligands are those ligands containing two or more chemically different atoms or groups of atoms suitable for coordination to a metal center. In addition, hybrid ligands frequently contain functionalities that display hemilabile² properties. Hemilabile atoms or groups of atoms can reversibly create or occupy a vacant coordination site on a transition metal center. Therefore, hybrid, hemilabile ligands may enhance selectivity in catalytic systems, or stabilize reactive intermediates.^{1–3} Transition metal complexes containing hemilabile, bidentate phosphines fall into these categories. Systems such as phosphinoether, -amine, and -ester ligands are known to exhibit

hemilabile properties.^{2a–i} For example, Werner and co-workers have demonstrated the hemilabile properties of the hybrid $\text{Pr}_2\text{PCH}_2\text{CH}_2\text{OMe}$ ligand when bound to ruthenium(II) in the complex $[\text{RuCl}_2(\eta^2\text{-Pr}_2\text{PCH}_2\text{CH}_2\text{OMe})_2]$, by displacement of the metal–O bond with CO and $\text{HC}\equiv\text{CPh}$.^{2b} The $\text{Pr}_2\text{PCH}_2\text{CO}_2\text{Me}$ ligand gave similar results with CO and terminal acetylenes when bound to ruthenium(II) in the $[(\eta^5\text{-C}_5\text{Me}_5)\text{RuCl}\{\eta^2\text{-}(P,O)\text{-Pr}_2\text{PCH}_2\text{CO}_2\text{Me}\}]\text{PF}_6$ compound.^{2g} The $\text{Pr}_2\text{PCH}_2\text{CH}_2\text{OMe}$ ligand, when bound to an iridium precatalyst, exhibited hemilabile properties when used in the hydrogenation of phenylacetylene.^{2d} Finally, Shell used a hybrid, hemilabile phosphine ligand bound to nickel for the commercial oligomerization of ethylene to prepare linear α -olefins.^{2i–k}

Our investigations with olefinic phosphines, specifically diphenylvinylphosphine (DPVP), resulted in the synthesis of $[(\eta^5\text{-C}_5\text{H}_5)\text{Ru}(\eta^3\text{-DPVP})(\eta^1\text{-DPVP})]\text{PF}_6$ (**A**).⁴ **A** contains the η^3 -DPVP ligand, which is a neutral, monometallic phosphaallyl ligand. The hemilabile character of the phosphaallyl ligand illustrated as the metal-bound vinyl group was readily displaced by carbon monoxide, nitriles, isonitriles, and phosphines (see Chart 1). In continuing efforts to explore olefinic phosphines as hemilabile ligands, we have prepared **1**, $[(\eta^5\text{-C}_5\text{Me}_5)\text{Ru}(\eta^3\text{-DPVP})(\eta^1\text{-DPVP})]\text{PF}_6$, the electron-rich analog of **A**. To the best of our knowledge, **1**

[†] University of Nevada—Reno.

[‡] Université Louis Pasteur.

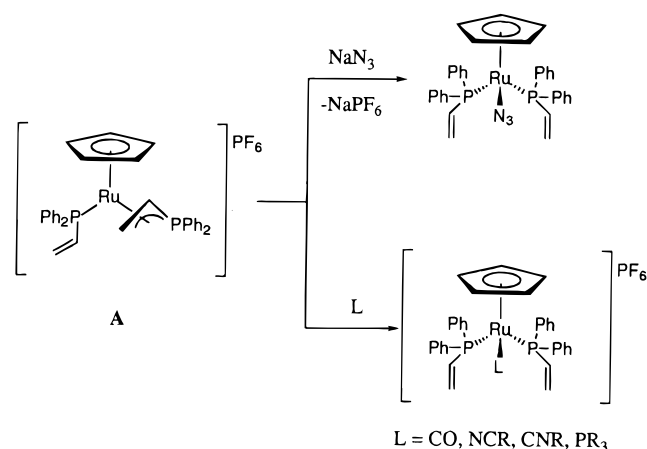
[®] Abstract published in *Advance ACS Abstracts*, April 1, 1997.

(1) (a) Lindner, E.; Bader, A. *Coord. Chem. Rev.* **1991**, *108*, 27. (b) Podlahová, J.; Kratochvíl, B.; Langer, V. *Inorg. Chem.* **1981**, *20*, 2160. (2) (a) Jeffrey, J. C.; Rauchfuss, T. B. *Inorg. Chem.* **1979**, *18*, 2658. (b) Martín, M.; Gevert, O.; Werner, H. *J. Chem. Soc., Dalton Trans.* **1996**, 2275, and references therein. (c) Werner, H.; Stark, A.; Schulz, M.; Wolf, J. *Organometallics* **1992**, *11*, 1126. (d) Esteruelas, M. A.; López, A. M.; Oro, L. A.; Pérez, A.; Schulz, M.; Werner, H. *Organometallics* **1993**, *12*, 1823. (e) Mason, M. R.; Verkade, J. G. *Organometallics* **1992**, *11*, 1514. (f) Sassano, C. A.; Mirkin, C. A. *J. Am. Chem. Soc.* **1995**, *117*, 11379. (g) Lindner, E.; Haustein, M.; Fawzi, R.; Steimann, M.; Wenger, P. *Organometallics* **1994**, *13*, 5021. (h) Braun, T.; Steinert, P.; Werner, H. *J. Organomet. Chem.* **1995**, *488*, 169. (i) Parshall, G. W.; Ittel, S. D. *Homogeneous Catalysis: The Applications and Chemistry of Catalysts by Soluble Transition Metal Complexes*, 2nd ed.; Wiley Interscience: New York, **1992**; pp 70–72. (j) Keim, W. *Angew. Chem., Int. Ed. Engl.* **1990**, *29*, 235. (k) Andrieu, J.; Braunstein, P.; Naud, F.; Adams, R. D.; Layland, R. *Bull. Soc. Chim. Fr.* **1996**, *133*, 669.

(3) (a) Adams, H.; Bailey, N. A.; Colley, M.; Schofield, P. A.; White, C. *J. Chem. Soc., Dalton Trans.* **1994**, 1445. (b) Jutzi, P.; Kristen, M. O.; Dahlhaus, J.; Neumann, B.; Stammli, H.-G. *Organometallics* **1993**, *12*, 2980. (c) Okuda, J.; Zimmermann, K. H. *Angew. Chem., Int. Ed. Engl.* **1991**, *30*, 430. (d) Jutzi, P.; Redeker, T.; Neumann, B.; Stammli, H.-G. *Organometallics* **1996**, *15*, 4153.

(4) Ji, H.-L.; Nelson, J. H.; DeCain, A.; Fischer, J.; Solujić, L.; Milosavljević, E. B. *Organometallics* **1992**, *11*, 401.

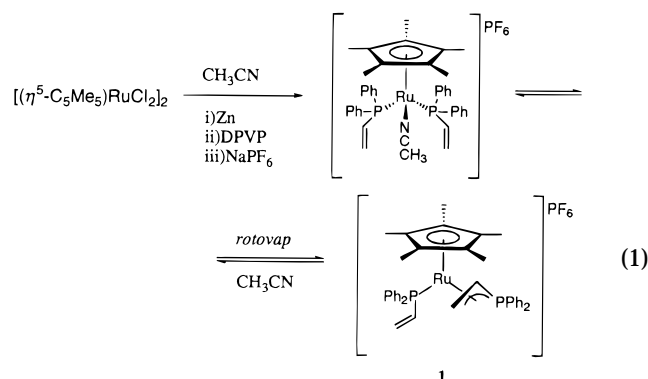
Chart 1. Reactions of the Phosphaallyl Ligand



represents only the second example⁴ of a neutral, monometallic phosphaallyl. An abstract of the X-ray crystal structure of **1** has appeared.⁵ Herein we report the synthesis, full details of the crystal structure, and the reactivity of **1** to probe the hemilabile properties of this system. Reactions of **1** with sodium thiocyanate, carbon monoxide, phenylacetylene, propargyl alcohol, and 3-butyn-1-ol are discussed.

Results and Discussion

Synthesis and Characterization of $[(\eta^5\text{-C}_5\text{Me}_5)\text{Ru}(\eta^3\text{-DPVP})(\eta^1\text{-DPVP})\text{PF}_6]$ (1**).** The preparation of **1** is accomplished by modification of the procedure described by Balavoine.⁶ In acetonitrile, a deep red solution of $[(\eta^5\text{-C}_5\text{Me}_5)\text{RuCl}_2]_2$ is treated with excess powdered zinc and the solution gradually turns yellow/brown. After 2 h, the excess zinc is removed by filtration and the solution is treated with DPVP for 8 hours at room temperature. The resulting solution is then treated with sodium hexafluorophosphate to produce **1** in 72% yield after recrystallization (eq 1). **1** is a



bright yellow, crystalline material that is air stable both in the solid state and in aerated solutions. Similar to what is observed for **A**, **1** reversibly binds acetonitrile; however, in contrast to **A**, **1** reacts with acetonitrile more slowly. Another notable difference between the two compounds is that coordinated acetonitrile is quantitatively removed from **1** on a rotary evaporator (~ 10 mmHg) under mild conditions ($\sim 40^\circ\text{C}$, 15 min). In

Chart 2

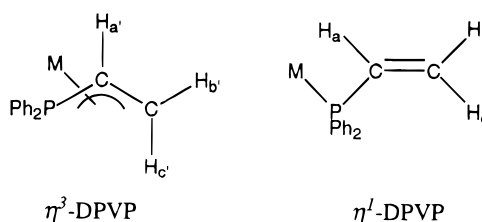


Table 1. ^1H NMR Data of **1** and **A**⁴ for the η^3 - and η^1 -DPVP Ligands^a

cmplx		η^3 -DPVP			η^1 -DPVP		
		$\text{H}_{a'}$	$\text{H}_{b'}$	$\text{H}_{c'}$	H_a	H_b	H_c
A	δ	4.08	4.06	2.41	4.54	5.61	5.12
	m	m	m	m	ddd	ddd	ddd
	$^3J(\text{PH})$	15.03 ^b	22.24	21.94	$^3J(\text{PH})$	25.24 ^b	37.57
	$^3J(\text{PH})$	10.52	4.51	10.52			
	$^3J(a'b')^c$	8.65	8.65		$^3J(\text{ac})$	18.33	18.33
	$^3J(a'c')$	6.1		6.1	$^3J(\text{ab})$	12.32	12.32
1	δ	3.12	3.20	2.62	4.25	5.35	5.03
	m	m	m	m	ddd	ddd	ddd
	$^3J(\text{PH})$	13.22 ^b	34.86	16.23	$^3J(\text{PH})$	26.15 ^b	36.06
	$^3J(\text{PH})$	2.10	1.80	6.31			
	$^3J(a'b')$	10.37	10.37		$^3J(\text{ac})$	17.43	17.43
	$^3J(a'c')$	0.62		0.62	$^3J(\text{ab})$	12.32	12.32
	$^2J(b'c')$		9.91	9.91	$^2J(\text{bc})$	0.60	0.60

^a NMR spectra measured in CDCl_3 . All chemical shifts are reported in ppm downfield from tetramethylsilane. All coupling constants are reported in hertz. ^b $^2J(\text{PH})$. ^c $^3J(\text{HH})$ coupling where the symbols a' , b' , c' , a , b , and c represent $\text{H}_{a'}$, $\text{H}_{b'}$, $\text{H}_{c'}$, H_a , H_b , and H_c , respectively, as defined in Chart 2.

contrast, quantitative removal of acetonitrile from **A** requires heating at $70\text{--}75^\circ\text{C}$ under high vacuum (0.5 mmHg) for several days.⁴ The relative ease with which acetonitrile is removed from **1** is attributed to an enhanced ruthenium–phosphaallyl π -backbonding interaction as a result of the strong electron-donating ability of the $\eta^5\text{-C}_5\text{Me}_5$ ligand. The $^{31}\text{P}\{^1\text{H}\}$ NMR spectrum of **1** in chloroform-*d* shows two doublets corresponding to the two inequivalent phosphines at 44.8 and 14.3 ppm with a coupling constant of $^2J_{\text{PP}} = 48.5$ Hz. On the basis of the assignment of the $^{31}\text{P}\{^1\text{H}\}$ NMR spectrum of **A**, the η^1 -DPVP and η^3 -DPVP phosphorus nuclei resonate at 44.8 and 14.3 ppm, respectively. This assignment was confirmed by selective $^1\text{H}\{^{31}\text{P}\}$ NMR spectroscopy. In addition, the phosphorus chemical shifts of **1** are similar to those of **A**, which shows two doublets at 42.3 and 24.2 ppm ($^2J_{\text{PP}} = 43.9$ Hz), respectively.⁴ The ^1H NMR spectrum of **1** shows three multiplets corresponding to the η^1 -DPVP hydrogens at 5.35, 5.03, and 4.25 ppm for H_b , H_c , and H_a protons, respectively (see Chart 2). The η^3 -DPVP phosphaallyl hydrogens resonate at 3.20, 2.62, and 3.12 ppm for $\text{H}_{b'}$, $\text{H}_{c'}$ and $\text{H}_{a'}$ respectively, and appear as complex multiplets. All aspects of the ^1H NMR spectral data for **1** are comparable to those of **A**,⁴ and Table 1 summarizes selected ^1H NMR data for both compounds. Moreover, the η^3 -DPVP ligand is bound in the *exo* orientation both in solution and in the solid state, as confirmed by a 1D-NOE difference experiment and X-ray crystallography.

A view of the geometry of the cation of **1** is shown in Figure 1. Selected bond distances and angles are listed in Table 2. Crystallographic data and details of structure determination are given in Table 6. The analysis reveals a distorted octahedral geometry at ruthenium; the $\eta^5\text{-C}_5\text{Me}_5$ moiety occupies three facial coordination

(5) Barthel-Rosa, L. P.; Nelson, J. H.; Catalano, V. J.; Fischer, J. *Phosphorus, Sulfur, Silicon* **1996**, 109–110, 169–172.

(6) Balavoine, G. G. A.; Boyer, T. *Organometallics* **1992**, 11, 456.

(7) Koelle, U.; Kossakowski, J. *Inorg. Synth.* **1992**, 29, 225–228.

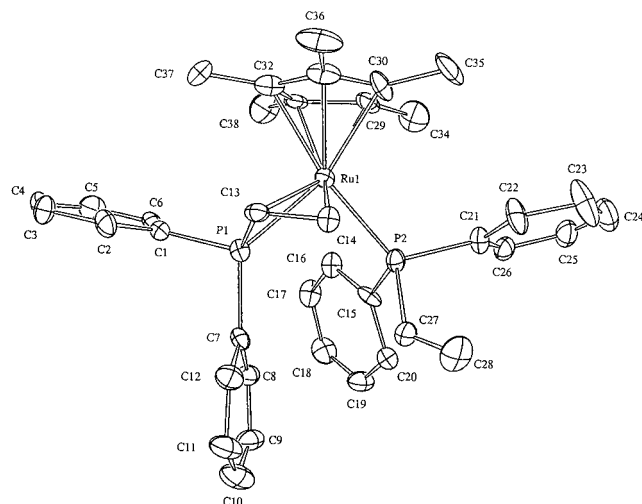


Figure 1. Structural drawing of one cation of $[(\eta^5\text{-C}_5\text{Me}_5)\text{-Ru}(\eta^3\text{-DPVP})(\eta^1\text{-DPVP})]\text{PF}_6$ (**1**) showing the atom numbering scheme (30% probability ellipsoids). Hydrogen atoms have been omitted for clarity.

Table 2. Selected Bond Distances and Angles for Cation **1** of $[(\eta^5\text{-C}_5\text{Me}_5)\text{Ru}(\eta^3\text{-DPVP})(\eta^1\text{-DPVP})]\text{PF}_6$ (**1**)

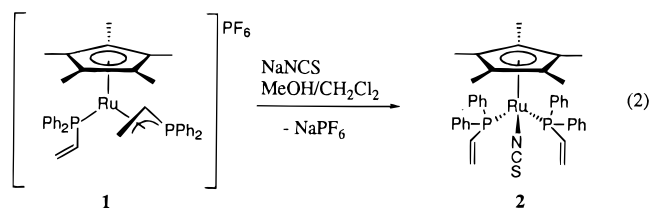
Bond Distances (Å)			
Ru1–P1	2.288(4)	Ru1–C14	2.25(2)
Ru1–P2	2.355(5)	Ru1–C29	2.30(2)
P1–C13	1.71(2)	Ru1–C30	2.23(2)
P2–C27	1.84(2)	Ru1–C31	2.20(2)
C13–C14	1.51(3)	Ru1–C32	2.26(2)
C27–C28	1.24(2)	Ru1–C33	2.31(2)
Ru1–C13	2.17(2)	Ru1–Cp ^a	1.90
Bond Angles (deg)			
P1–Ru1–P2	91.1(2)	C1–P1–C7	104.6(6)
P1–Ru1–C13	44.9(5)	C15–P2–C21	104.0(8)
P1–Ru1–C14	75.0(4)	C1–P1–C13	110.0(8)
Ru1–P1–C13	63.9(6)	C15–P2–C27	100.3(8)
Ru1–P2–C27	117.6(6)	C7–P1–C13	112.9(8)
P1–C13–C14	118(1)	C21–P2–C27	101.2(7)
P2–C27–C28	129(2)		

^a Cp^a denotes the centroid of the C29–C33 ring.

sites, with one η^1 -DPVP and one η^3 -DPVP completing the coordination sphere. There are no unusual interionic contacts. There are two molecules in the asymmetric unit, and the cations have an enantiomeric relationship. The metrical parameters for the two cations are very similar, and the discussion that follows is for only one of them. Complete data are given in the Supporting Information. For **1**, the η^3 -DPVP ligand has a Ru1–P1 bond distance of 2.288(4) Å, and the η^1 -DPVP ligand has a longer Ru1–P2 bond distance of 2.355(5) Å while the P1–Ru1–P2 bond angle is 91.1(2)°. Both Ru–P distances in **1** are very similar to the analogous distances of 2.276(1) and 2.315(1) Å for **A**, which has a P–Ru–P bond angle of 93.34(3)°. For **1**, the η^3 -DPVP phosphaaallyl ligand has a P1–C13 bond distance of 1.71(2) Å, which is shorter than the P2–C27 bond distance of 1.84(2) Å for the η^1 -DPVP vinylphosphine ligand. The same trends are observed for **A**, which has P–C bond distances of 1.761(4) and 1.810(3) Å for the η^3 -DPVP and η^1 -DPVP ligands, respectively. For **1**, the coordinated C13–C14 bond of the η^3 -DPVP ligand has a distance of 1.51(3) Å, which is significantly longer than the C27–C28 bond distance of 1.24(2) Å for the η^1 -DPVP ligand. The same trends are observed for **A**, which has C–C bond distances of 1.399(5) and 1.306(5) Å for the

η^3 -DPVP and η^1 -DPVP ligands, respectively. The coordinated C13–C14 bond distance in **1** (1.51 Å) is significantly longer than the analogous coordinated C–C bond in **A** (1.399 Å). The longer coordinated C–C bond distance in **1** compared to that of **A** is attributed to the more electron-rich ruthenium center in **1** as a result of the strong electron-donating properties of the η^5 -C₅Me₅ ligand. The Ru1–C13 and Ru1–C14 bond distances of 2.17(2) and 2.25(2) Å in **1** are virtually identical to the respective metal–carbon bond distances of 2.176(3) and 2.244(4) Å for **A**. The similar metal–carbon bond distances of the η^3 -DPVP ligands in **1** and **A** are not surprising, since those distances have little dependence on the electron density at ruthenium. Overall, the crystallographic data for **1** confirms the phosphaaallyl nature of the η^3 -DPVP ligand.

Reactions of 1. Treatment of a dichloromethane/methanol solution of **1** with a large excess of NaNCS at room temperature results in the formation of **2**, $[(\eta^5\text{-C}_5\text{Me}_5)\text{Ru}(\eta^1\text{-DPVP})_2(\text{NCS})]\text{PF}_6$ (eq 2). The η^3 -DPVP phos-

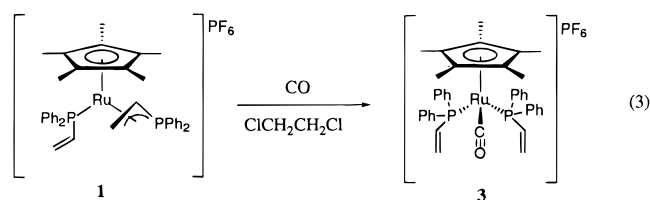


phaaallyl ligand is displaced by the incoming thiocyanate ion, which is confirmed by $^{31}\text{P}\{^1\text{H}\}$ NMR spectroscopy as the two doublets at 44 and 14 ppm disappear and a singlet appears at 39.0 ppm. The ^1H NMR spectrum in chloroform-*d* shows complex multiplets at 5.69 and 5.19 ppm for the uncoordinated vinyl hydrogens, which is typical for disubstituted metal–DPVP complexes.^{4,8} Second-order effects arising from coupling to both phosphorus nuclei give rise to the complex nature of the vinyl resonances. The resonance for the η^5 -C₅Me₅ hydrogens appears as a triplet at 1.33 ppm ($^4J_{\text{PH}} = 1.5$ Hz). Both the $^{31}\text{P}\{^1\text{H}\}$ and ^1H NMR spectroscopic data indicate that **2** contains a mirror plane of symmetry in solution with two η^1 -DPVP ligands. The IR spectrum of **2** in Nujol shows characteristic $\nu(\text{N}=\text{CS})$ at 2095 cm^{-1} and $\nu(\text{NCS})$ at 800 cm^{-1} , indicating that the thiocyanate ligand is bound through the nitrogen atom.⁹ The most notable feature of the $^{13}\text{C}\{^1\text{H}\}$ NMR spectrum in chloroform-*d* is the presence of the NCS carbon resonance as a triplet at 127.17 ppm ($^3J_{\text{PC}} = 1.9$ Hz). Both the IR and $^{13}\text{C}\{^1\text{H}\}$ NMR data are characteristic of an N-bound NCS[−] moiety.⁹ Treatment of **1** with NaN₃ under similar conditions led to the formation of many products, as indicated by $^{31}\text{P}\{^1\text{H}\}$ NMR spectroscopy, with resonances of approximately equal intensity at 38.7, 37.3, 31.1, and 24.4 ppm. In addition, these solutions are air sensitive and decompose rapidly. No further attempts were made to purify the compound(s) formed in the NaN₃ reaction.

(8) Barthel-Rosa, L. P.; Catalano, V. J.; Maitra, K.; Nelson, J. H. *Organometallics* **1996**, *15*, 3924.

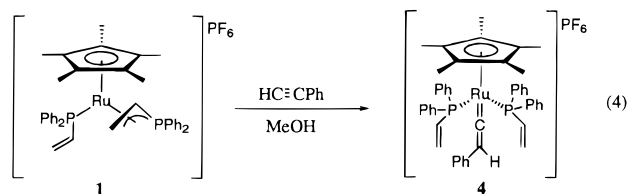
(9) (a) MacDougall, J. J.; Nelson, J. H.; Fultz, W. C.; Burmeister, J. L.; Holt, E. M.; Alcock, N. W. *Inorg. Chim. Acta* **1982**, *63*, 75. (b) Nelson, J. H.; MacDougall, J. J.; Alcock, N. W.; Mathey, F. *Inorg. Chem.* **1982**, *21*, 1200. (c) Fultz, W. C.; Burmeister, J. L.; MacDougall, J. J.; Nelson, J. H. *Inorg. Chem.* **1980**, *19*, 1085. (d) For S-bound ruthenium NCS[−] complex, see: Homanen, P.; Haukka, M.; Pakkanen, T. A.; Pursiainen, J.; Laitinen, R. H. *Organometallics* **1996**, *15*, 4081.

Treatment of **1** with CO in refluxing 1,2-dichloroethane results in the formation of the bright yellow **3**, $[(\eta^5\text{-C}_5\text{Me}_5)\text{Ru}(\eta^1\text{-DPVP})_2(\text{CO})]\text{PF}_6$, in high yield after 116 h (eq 3). The $^{31}\text{P}\{^1\text{H}\}$ NMR spectrum in chloro-



form-*d* shows a singlet at 35.3 ppm while the ^1H NMR spectrum shows the characteristic second-order uncoordinated vinyl hydrogen resonances at 5.93, 5.45, and 5.29 ppm. The $^{13}\text{C}\{^1\text{H}\}$ NMR spectrum shows the characteristic triplet at 204.25 ppm ($^2J_{\text{CP}} = 17.2$ Hz) for the carbonyl carbon. For $[(\eta^5\text{-C}_5\text{H}_5)\text{Ru}(\eta^1\text{-DPVP})_2(\text{CO})]\text{PF}_6$, the CO carbon resonance occurs at 202.68 ppm ($^2J_{\text{PC}} = 17.3$ Hz) in nitromethane-*d*₃.⁴ Substitution of CO onto **1** to form **3** required a much longer reaction time (116 h) when compared to the $\eta^5\text{-C}_5\text{H}_5$ analog **A** (8 h), under similar conditions. The long reaction time for the conversion of **1** into **3** is attributed to a stronger ruthenium η^3 -DPVP phosphaallyl interaction as a result of the electron-donating properties of the $\eta^5\text{-C}_5\text{Me}_5$ ligand compared to $\eta^5\text{-C}_5\text{H}_5$.

Other illustrative examples of the hemilabile properties of the η^3 -DPVP phosphaallyl ligand are the reactions with terminal acetylenes. Treatment of **1** with phenylacetylene in refluxing methanol affords the vinylidene **4**, $[(\eta^5\text{-C}_5\text{Me}_5)\text{Ru}(\eta^1\text{-DPVP})_2\{\text{C}=\text{C}(\text{H})(\text{Ph})\}]\text{PF}_6$ (eq 4). The $^{31}\text{P}\{^1\text{H}\}$ NMR spectrum in chloroform-*d*



shows a singlet at 38.0 ppm while the ^1H NMR spectrum shows the characteristic second-order uncoordinated vinyl hydrogen resonances at 5.79, 5.65, and 5.01 ppm. The unique vinylidene hydrogen resonance appears as a broad triplet at 5.26 ppm ($^4J_{\text{HP}} = 2.2$ Hz). The $^{13}\text{C}\{^1\text{H}\}$ NMR spectrum shows the characteristic $\text{Ru}=\text{C}_\alpha$ carbon resonance at 353.6 ppm, but the phosphorus-carbon coupling is not resolved. The NMR data for **4** compare with the values reported for $[(\eta^5\text{-C}_5\text{Me}_5)\text{Ru}(\text{PPhMe}_2)_2\{\text{C}=\text{C}(\text{H})(\text{Ph})\}]\text{PF}_6$, which shows the unique vinylidene hydrogen resonance as a triplet at 5.42 ppm ($^4J_{\text{HP}} = 2.2$ Hz) and the $\text{Ru}=\text{C}_\alpha$ carbon resonance at 354.3 ppm.¹⁰ In addition, the spectroscopic data for **1** are typical for transition metal vinylidene complexes.¹¹ **4** was also characterized by X-ray crystallography.

A view of the structure of the cation of **4** is shown in Figure 2. Selected bond distances and angles are listed in Table 3. The analysis reveals a distorted octahedral geometry about ruthenium with one $\eta^5\text{-C}_5\text{Me}_5$ moiety that occupies three facial coordination sites, two η^1 -DPVP ligands and the $\text{C}=\text{C}(\text{H})(\text{Ph})$ vinylidene moiety completing the coordination sphere. The interligand bond angles of $92.5(2)^\circ$ for P1-Ru1-P2 , $86.7(4)^\circ$ for C15-Ru1-P1 and $89.8(4)^\circ$ for C15-Ru1-P2 reflect the

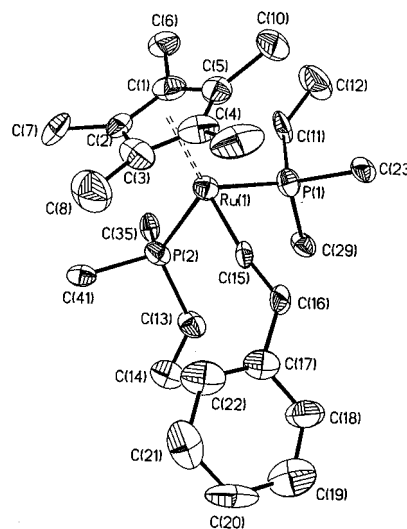


Figure 2. Structural drawing of the cation of $[(\eta^5\text{-C}_5\text{Me}_5)\text{Ru}(\eta^1\text{-DPVP})_2\{\text{C}=\text{C}(\text{H})(\text{Ph})\}]\text{PF}_6$ (**4**) showing the atom numbering scheme (40% probability ellipsoids). Hydrogen atoms and phenyl carbon atoms of the η^1 -DPVP ligands have been omitted for clarity.

Table 3. Selected Bond Distances and Angles for $[(\eta^5\text{-C}_5\text{Me}_5)\text{Ru}(\eta^1\text{-DPVP})_2\{\text{C}=\text{C}(\text{H})(\text{Ph})\}]\text{PF}_6$ (**4**)

Bond Distances (Å)			
Ru1-P1	2.346(4)	C13-C14	1.29(2)
Ru1-P2	2.355(3)	Ru1-C1	2.330(14)
Ru1-C15	1.824(13)	Ru1-C2	2.336(13)
C15-C16	1.33(2)	Ru1-C3	2.263(14)
C16-C17	1.47(2)	Ru1-C4	2.271(13)
P1-C11	1.797(12)	Ru1-C5	2.268(13)
P2-C13	1.83(2)	Ru1-Cp ^a	1.954
C11-C12	1.29(2)		
Bond Angles (deg)			
P1-Ru1-P2	92.5(2)	C11-P1-Ru1	113.9(5)
C15-Ru1-P1	86.7(4)	C13-P2-Ru1	115.1(5)
C15-Ru1-P2	89.8(4)	C12-C11-P1	126.7(13)
C16-C15-Ru1	172.5(11)	C14-C13-P2	128(2)
C15-C16-C17	128.4(13)		

^a Cp^{*} denotes the centroid of the C(1-5) ring.

distorted octahedral geometry at ruthenium. The Ru1-C15 bond length is 1.824(13) Å while the C15-C16 length is 1.33(2) Å, which are typical values for vinylideneruthenium complexes.^{10,11} The vinylidene ligand is nearly linear with a C16-C15-Ru1 bond angle of $172.5(11)^\circ$ which is only slightly smaller than the angle of $174(1)^\circ$ reported for $[(\eta^5\text{-C}_5\text{Me}_5)\text{Ru}(\text{PPhMe}_2)_2\{\text{C}=\text{C}(\text{H})(\text{Ph})\}]\text{PF}_6$.¹⁰ In **4**, the vinylidene plane defined by Ru1-C15-C16-C17 makes an angle of 87.6° with the plane bisecting the P1-Ru-P2 angle, which is typical for half-sandwich vinylidene complexes.^{11,12} Kostic and Fenske calculated that maximal π -stabilization arises when the p orbitals of the C_α carbon and the metal $2a''$ orbital interact with one another,¹³ a consistent with the observed orientation of the vinylidene fragment in **4**. However, there exists a second, lower energy π interaction between the π^* orbital of the organic group and the

(10) Lagadee, R. L.; Roman, E.; Toupet, L.; Müller, U.; Dixneuf, P. H. *Organometallics* **1994**, *13*, 5030.

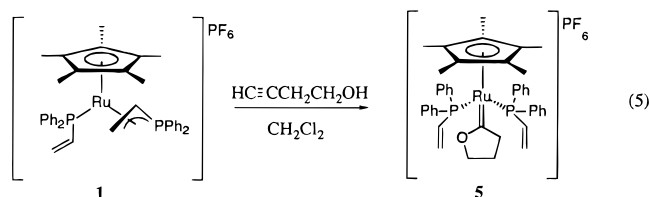
(11) Bruce, M. I. *Chem. Rev.* **1991**, *91*, 197.

(12) Davies, S. G.; McNally, J. P.; Smallridge, A. J. *Adv. Organomet. Chem.* **1990**, *30*, 1.

(13) (a) Kostic, N. M.; Fenske, R. F. *Organometallics* **1982**, *1*, 974. (b) Schilling, B. E. R.; Hoffman, R.; Lichtenberger, D. L. *J. Am. Chem. Soc.* **1979**, *101*, 585. (c) Consiglio, G.; Morandini, F. *Inorg. Chim. Acta* **1987**, *127*, 79. (d) Consiglio, G.; Bangerter, F.; Darpin, C.; Morandini, F.; Lucchini, V. *Organometallics* **1984**, *3*, 1446.

metal fragment 3a' orbital, which predicts facile rotation about the metal–C $_{\alpha}$ (M=C $_{\alpha}$) bond.¹² The barrier to rotation about metal–vinylidene (M=C $_{\alpha}$) bonds has been calculated to be on the order of 15 kJ/mol.^{13b} This barrier was measured to be around 38–43 kJ/mol for a series of ruthenium(II) vinylidene compounds of the type, $[(\eta^5\text{-C}_5\text{H}_5)\text{-Ru}(\text{Ph}_2\text{PCHRCHR}'\text{PPh}_2)\{\text{C}=\text{C}(\text{H})\text{-}(\text{R}')\}]^+$.^{11–13c,d}

Treatment of **1** with 3-butyne-1-ol in refluxing dichloromethane affords the cyclic Fischer carbene complex **5**, $[(\eta^5\text{-C}_5\text{Me}_5)\text{Ru}(\eta^1\text{-DPVP})_2\{\text{C}(\text{CH}_2)_3\text{O}\}]\text{PF}_6$ (eq 5). The



$^{31}\text{P}\{^1\text{H}\}$ NMR spectrum in dichloromethane shows that the first step in the reaction is isomerization of the alkene to form the metal–vinylidene,¹² which appears as a singlet at 38 ppm. No attempt was made to isolate the intermediate vinylidene compound. Upon heating, intramolecular attack of the hydroxyl group at the Ru=C $_{\alpha}$ carbon, concomitant with a proton shift, results in the formation of the final product **5**. The synthesis of cyclic carbenes by metal-mediated activation of 3-butyne-1-ol has been used to make close analogs of **5** including the following: $[(\eta^5\text{-C}_5\text{H}_5)\text{Ru}(\text{PMe}_3)_2\{\text{C}(\text{CH}_2)_3\text{O}\}]^+$,¹⁴ $[(\eta^5\text{-C}_5\text{H}_5)\text{Ru}(\text{PPh}_3)_2\{\text{C}(\text{CH}_2)_3\text{O}\}]^+$,¹⁵ and $[(\eta^6\text{-C}_6\text{Me}_6)\text{Ru}(\text{PMe}_3)(\text{Cl})\{\text{C}(\text{CH}_2)_3\text{O}\}]^+$.¹⁶ The notable features of the ^1H NMR spectrum of **5** (in chloroform-*d*) include two triplets at 4.31 and 3.35 ppm ($^3J_{\text{HH}} = 7.0$ Hz) and a broad multiplet at 2.11 ppm for the hydrogens of the three methylene groups in the carbene ring. The ^1H NMR spectral features of **5** compare to those of $[(\eta^5\text{-C}_5\text{H}_5)\text{Ru}(\text{PPh}_3)_2\{\text{C}(\text{CH}_2)_3\text{O}\}]^+$,¹⁴ which shows two triplets at 3.93 and 3.74 ppm and a quintet at 1.77 ppm ($^3J_{\text{HH}} = 8$ Hz) for the methylene protons of the carbene ring. The $^{31}\text{P}\{^1\text{H}\}$ NMR spectrum of **5** in chloroform-*d* consists of a singlet at 45.1 ppm while the $^{13}\text{C}\{^1\text{H}\}$ NMR spectrum shows the carbene carbon (Ru=C $_{\alpha}$) resonance at 299.5 ppm; however, the triplet structure due to phosphorus coupling was not completely resolved. The methylene carbons of the carbene ring resonate as singlets at 80.86, 55.81, and 23.41 ppm. The $^{13}\text{C}\{^1\text{H}\}$ NMR spectrum of $[(\eta^5\text{-C}_5\text{H}_5)\text{Ru}(\text{PPh}_3)_2\{\text{C}(\text{CH}_2)_3\text{O}\}]^+$ ¹⁴ shows the resonance for the carbene carbon as a triplet at 300.5 ppm ($^2J(\text{PC}) = 14$ Hz) while the carbene ring carbons appear at 81.6, 60.8, and 22.6 ppm, all of which are typical values for these types of ruthenium carbenes.^{14–16}

5 was characterized by X-ray crystallography, and a view of the structure of the cation is shown in Figure 3. Selected bond distances and angles are listed in Table

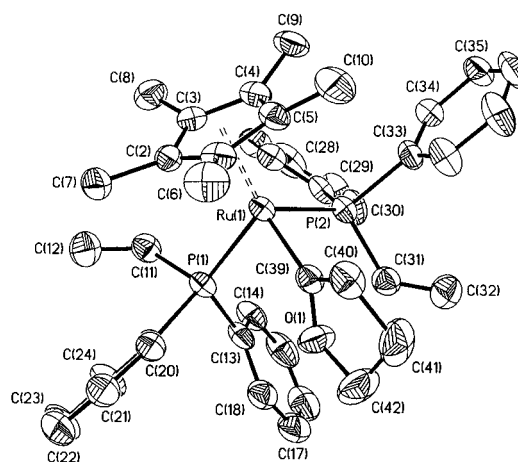


Figure 3. Structural drawing of the cation of $[(\eta^5\text{-C}_5\text{Me}_5)\text{-Ru}(\eta^1\text{-DPVP})_2\{\text{C}(\text{CH}_2)_3\text{OP}\}]\text{PF}_6$ (**5**) showing the atom numbering scheme (40% probability ellipsoids). Hydrogen atoms omitted for clarity.

Table 4. Selected Bond Distances and Angles for $[(\eta^5\text{-C}_5\text{Me}_5)\text{Ru}(\eta^1\text{-DPVP})_2\{\text{C}(\text{CH}_2)_3\text{O}\}]\text{PF}_6$ (**5**)

Bond Distances (Å)			
Ru1–P1	2.3270(13)	P2–C31	1.813(5)
Ru1–P2	2.3382(13)	C11–C12	1.318(7)
Ru1–C39	1.942(5)	C31–C32	1.303(7)
O1–C39	1.329(6)	Ru1–C1	2.283(5)
O1–C42	1.462(6)	Ru1–C2	2.272(5)
C41–C42	1.454(9)	Ru1–C3	2.341(5)
C40–C41	1.520(8)	Ru1–C4	2.328(5)
C39–C40	1.492(7)	Ru1–C5	2.298(5)
P1–C11	1.825(5)	Ru1–Cp* ^a	1.960
Bond Angles (deg)			
P1–Ru1–P2	94.41(5)	O1–C39–C40	107.0(4)
C39–Ru1–P1	90.1(2)	C39–C40–C41	103.8(5)
C39–Ru1–P2	87.38(14)	C42–C41–C40	103.1(5)
O1–C39–Ru1	123.2(3)	C41–C42–O1	104.3(5)
C40–C39–Ru1	129.8(4)	C39–O1–C42	112.6(4)

^a Cp* denotes the centroid of the C(1–5) ring.

4. The analysis reveals a distorted octahedral coordination geometry about ruthenium with one facial $\eta^5\text{-C}_5\text{-Me}_5$ moiety, two $\eta^1\text{-DPVP}$ ligands, and the cyclic carbene moiety completing the coordination sphere. The interligand bond angles of 94.41(5)° for P1–Ru1–P2, 90.1(2)° for C39–Ru1–P1 and 87.38(14)° for C39–Ru1–P2 reflect the distorted octahedral geometry at ruthenium. There are two molecules in the asymmetric unit that differ only in the conformations of the cyclic carbene ring. Both molecules have essentially the same geometrical shape; therefore, only the distances and angles of one of them will be discussed. The Ru1–C39 distance in **5** is 1.942(5) Å, which compares with the ruthenium carbene carbon bond length of 1.946(8) Å in the analogous ruthenium compound $[(\eta^5\text{-C}_5\text{H}_5)(\text{CO})(\text{PPh}_3)\text{Ru}\{\text{C}(\text{CHPh})(\text{CH}_2)_2\text{O}\}]^+$,^{17a} and falls between the metal carbene bond distances of 2.086(8), 1.889(8), and 2.00–(2) Å for $[(\eta^5\text{-C}_5\text{H}_5)(\text{CO})_2(\text{I})\text{Mo}\{\text{C}(\text{CH}_2)_3\text{O}\}]$,^{17b} $[(\text{CO})_4\text{Mn}(\mu\text{-I})\text{Pt}\{\text{C}(\text{CH}_2)_3\text{O}\}(\text{PBu}_2\text{Me})]$,^{17c} and $[(\text{CH}_3)(\text{PMe}_2\text{Ph})_2\text{Pt}$

(14) Bruce, M. I.; Swincer, A. G.; Thomson, B. J.; Wallis, R. C. *Aust. J. Chem.* **1980**, *33*, 2605.

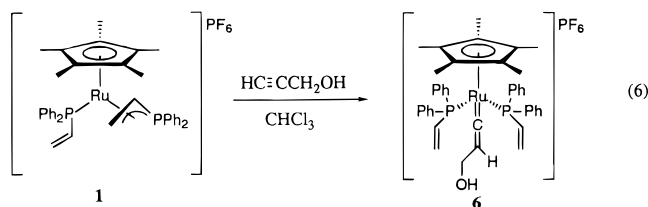
(15) Gamasa, M. P.; Gimeno, J.; Gonzalez-Cueva, M.; Lastra, E. *J. Chem. Soc., Dalton Trans.* **1996**, 2547.

(16) Bozec, H. L.; Ouzzine, K.; Dixneuf, P. H. *Organometallics* **1991**, *10*, 2768.

(17) (a) Nombel, P.; Lugan, N.; Mathieu, R. *J. Organomet. Chem.* **1995**, *503*, C22. (b) Bailey, N. A.; Chell, P. L.; Manuel, C. P.; Mukhopadhyay, A.; Rogers, D.; Tabbrown, H. E.; Winter, M. J. *J. Chem. Soc., Dalton Trans.* **1983**, 2397. (c) Berry, M.; Martin-Gil, J.; Howard, J. A. K.; Stone, F. G. A. *J. Chem. Soc., Dalton Trans.* **1980**, 1625. (d) Stephanick, R. F.; Payne, N. C. *J. Organomet. Chem.* **1974**, *72*, 453.

$\{\text{C}(\text{CH}_2)_3\text{O}\}$],^{17d} respectively. The C(39)–O(1) bond distance of 1.329(6) Å in **5** is very similar to the carbene carbon–oxygen bond distances of 1.312(9),^{17a} 1.337(11),^{17b} 1.32(1),^{17c} and 1.26(2) Å,^{17d} respectively, for the compounds listed above. The C40–C41 and C41–C42 bond distances of 1.520(8) and 1.454(9) Å are typical for C_{sp}^3 – C_{sp}^3 bond lengths. For **5**, the carbene ring adopts an envelope conformation and the deviations from the mean plane of the carbene ring defined by Ru1, C39, C40, and O1 are as follows: Ru1 –0.0012 Å, C39 0.0041 Å, C40 –0.0014 Å, C41 0.4963 Å, C42 0.0523 Å, and O1 –0.0014 Å. Deviations from planarity for these types of five-membered cyclic carbenes are not unusual, and the structures in the reported complexes above vary from nearly planar^{17c} to a deviation of –0.406 Å for the ring carbon β to the oxygen atom, O–CH₂–C β H₂.^{17b}

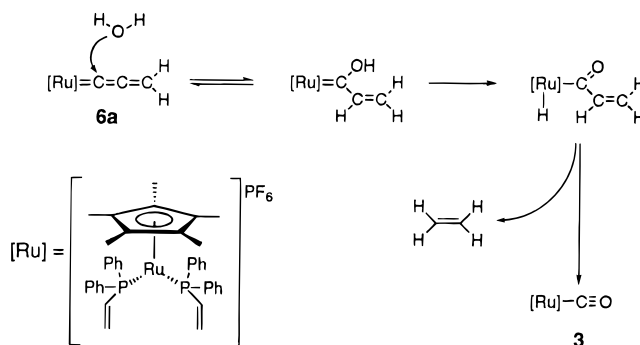
Treatment of **1** with propargyl alcohol in chloroform results in the formation of the vinylidene **6**, $[(\eta^5\text{-C}_5\text{Me}_5)\text{Ru}(\eta^1\text{-DPVP})_2\{\text{C}=\text{C}(\text{H})(\text{CH}_2\text{OH})\}]\text{PF}_6$ (eq 6). The



reaction requires 72 h to go to completion at room temperature. The $^{31}\text{P}\{^1\text{H}\}$ NMR spectrum of the reaction mixture (in chloroform) shows a resonance for **6** as a singlet at 38.6 ppm. Pure **6** is sparingly soluble in chloroform-*d*; therefore, ^1H and $^{13}\text{C}\{^1\text{H}\}$ NMR data were obtained in acetone-*d*₆. The ^1H NMR spectrum shows the unique vinylidene hydrogen resonance as a triplet of triplets at 4.88 ppm with coupling constants of $^3J_{\text{HH}} = 8.0$ Hz and $^4J_{\text{HP}} = 2.2$ Hz. The OH resonance appears as a triplet at 4.19 ppm ($^3J_{\text{HH}} = 5.8$ Hz), by virtue of the coupling to the CH₂ group. However, after 24 h at room temperature, the CH₂–OH coupling constant is washed out. The $^{13}\text{C}\{^1\text{H}\}$ NMR spectrum shows the vinylidene carbon (Ru=C α) as a triplet at 351.0 ppm ($^2J_{\text{CP}} = 15.7$ Hz) while the Ru=C=C β carbon resonates as a triplet at 112.8 ppm ($^3J_{\text{CP}} = 1.2$ Hz). The ^1H and $^{13}\text{C}\{^1\text{H}\}$ NMR spectral data for **6** are typical for vinylidenes¹¹ and very similar to the values reported for the close analog $[(\eta^5\text{-C}_5\text{Me}_5)(\text{PPhMe}_2)_2\text{Ru}\{\text{C}=\text{C}(\text{H})(\text{CH}_2\text{OH})\}]\text{PF}_6$,¹⁰ which shows the unique vinylidene hydrogen as a triplet of triplets at 4.63 ppm ($^3J_{\text{HH}} = 8.0$ Hz, $^4J_{\text{PH}} = 2.2$ Hz) and the triplet for the vinylidene Ru=C α at 346.4 ppm ($^2J_{\text{CP}} = 15.2$ Hz).

6 is a yellow-orange solid and forms orange solutions in acetonitrile, acetone, dichloromethane, and methanol. Upon standing for long periods of time, (>1 week), solutions of **6** gradually turn intensely violet. The violet color suggests that **6** gradually dehydrates to form the allenylidene complex, $[(\eta^5\text{-C}_5\text{Me}_5)\text{Ru}(\eta^1\text{-DPVP})_2\{\text{C}=\text{C}=\text{CH}_2\}]\text{PF}_6$ (**6a**), since solutions of many ruthenium allenylidene complexes^{18a–c} including the close analog, $[(\eta^6\text{-C}_6\text{Me}_6)\text{Ru}(\text{Cl})(\text{PMe}_3)\{\text{C}=\text{C}=\text{CPh}_2\}]\text{PF}_6$,^{18a} are violet

Scheme 1. Proposed Mechanism for the Transformation of Intermediate **6a** into **3**



in color. All attempts to isolate and purify the intermediate complex **6a** were not successful and ultimately resulted only in the isolation of the yellow carbonyl **3** (*vide supra*). The formation of **3** from solutions of **6/6a** suggests at least one possible decomposition pathway in which adventitious water attacks the Ru=C α carbon of the allenylidene to form an α,β -unsaturated hydroxycarbene, followed by hydrogen transfer to ruthenium with subsequent β -hydride elimination to give **3** and ethylene (Scheme 1). Although the intermediates proposed in Scheme 1 have not been directly observed, the nucleophilic addition of water at the Ru=C α carbon of allenylidenes to form hydroxycarbenes is known.^{19 a} Moreover, the hydration of vinylidenes into alkylcarbonyl compounds is well-known^{12,19b,c} and has recently been studied in detail.²¹ Therefore, the mechanism proposed for the transformation of **6** to **3** in Scheme 1 seems reasonable; however, a more meticulous investigation into this transformation is warranted.

Refluxing a solution of **6** in methanol over a period of several days resulted in the unexpected precipitation of a rose-colored solid. Recrystallization of the precipitate afforded X-ray quality crystals and a structural analysis was performed (*vide infra*). The structure was shown to be that of **7**, $[(\eta^5\text{-C}_5\text{Me}_5)\text{Ru}(\eta^1\text{-DPVP})_2\{\text{C}=\text{C}(\text{CH}_2)_2\text{PPh}_2\text{CH}_2\}]\text{PF}_6$ (Figure 4; Scheme 2). Compound **7** contains a novel heterocyclic, disubstituted vinylidene ($\text{C}=\text{CR}\sim\text{R}'$), where $\text{R}\sim\text{R}'$ is a *P,P*-diphenyl-trihydrophosphonium ring. Compound **7** "scavenged" DPVP from the solution, which then behaved as a nucleophile and attacked the allenylidene C γ carbon of the intermediate **6a** with concomitant ring closure to form a five-membered heterocycle. In the presence of excess DPVP and HPF₆, **6** readily reacts to form **7** as outlined in Scheme 2.

A very similar reaction was reported¹² for $[(\eta^5\text{-C}_5\text{H}_5)\text{Ru}(\text{PPh}_3)_2(\text{Cl})]$, a close analog of **1**. $[(\eta^5\text{-C}_5\text{H}_5)\text{Ru}(\text{PPh}_3)_2(\text{Cl})]$ was shown to react with propargyl alcohol and NH_4PF_6 to form the primary allenylidene complex $[(\eta^5\text{-C}_5\text{H}_5)(\text{PPh}_3)_2\text{Ru}\{\text{C}=\text{C}=\text{CH}_2\}]^+$, which then scav-

(18) (a) Bozec, H. L.; Ouzzine, K.; Dixneuf, P. H.; *J. Chem. Soc., Chem. Commun.* **1989**, 219. (b) Cadierno, V.; Gamasa, M. P.; Gimeno, J.; González-Cueva, M.; Lastra, E.; Borge, J.; García-Granda, S.; Pérez-Carreño E. *Organometallics* **1996**, *15*, 2137. (c) Pilette, D.; Ouzzine, K.; Le Bozec, H.; Dixneuf, P. H.; Rickard, C. E. F.; Roper, W. R. *Organometallics* **1992**, *11*, 809.

(19) (a) Esteruelas, M. A.; Gómez, A. V.; Lahoz, F. J.; López, A. M.; Oñate, E.; Oro, L. A. *Organometallics* **1996**, *15*, 3423. (b) Gamasa, M. P.; Gimeno, J.; Lastra, E.; Lanfranchi, M.; Tiripicchio, A. *J. Organomet. Chem.* **1992**, *430*, C39. (c) Bruce, M. I.; Swincer, A. G. *Aust. J. Chem.* **1980**, *33*, 1471.

(20) Bianchini, C.; Casares, J. A.; Peruzzini, M.; Romerosa, A.; Zanobini, F. *J. Am. Chem. Soc.* **1996**, *118*, 4585.

(21) (a) Cadierno, V.; Gamasa, M. P.; Gimeno, J.; Borge, J.; García-Granda, S. *J. Chem. Soc., Chem. Commun.* **1994**, 2495. (b) Cadierno, V.; Gamasa, M. P.; Gimeno, J.; Lastra, E. *J. Organomet. Chem.* **1994**, *474*, C27. (c) Berke, H.; Huttner, G.; Seyerl, J. *Z. Naturforsch.* **1981**, *36B*, 1277.

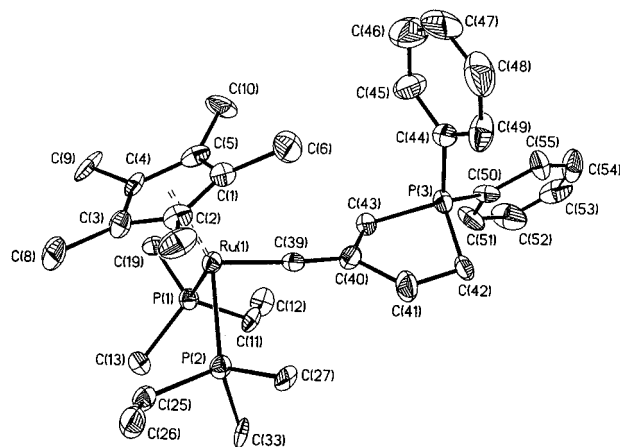
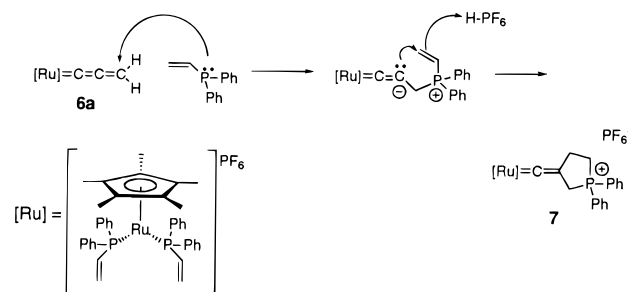


Figure 4. Structural drawing of the cation $[(\eta^5\text{-C}_5\text{-Me}_5)\text{Ru}(\eta^1\text{-DPVP})_2\{\text{C}=\text{C}(\text{CH}_2)_2\text{PPh}_2\text{CH}_2\}][\text{PF}_6]_2$ (**7**) showing the atom numbering scheme (30% probability ellipsoids). Hydrogen atoms and phenyl carbon atoms of the η^1 -DPVP ligands have been omitted for clarity.

Scheme 2. Possible Mechanism for the Formation of 7 from Intermediate 6a



enged PPh_3 to form the phosphonium salt, $[(\eta^5\text{-C}_5\text{H}_5)\text{Ru}(\text{PPh}_3)_2\{\text{C}=\text{C}(\text{CH}_2\text{PPh}_3)\}][\text{PF}_6]$.¹² The phosphonium salt was readily protonated with H-PF_6 to form the dicationic vinylidene compound $[(\eta^5\text{-C}_5\text{H}_5)\text{Ru}(\text{PPh}_3)_2\{\text{C}=\text{C}(\text{H})(\text{CH}_2\text{PPh}_3)\}][\text{PF}_6]_2$. MO calculations on the model compound, $[(\eta^5\text{-C}_5\text{H}_5)(\text{CO})_2\text{Mn}\{\text{C}=\text{C}=\text{CH}_2\}]$, have shown that the allenylidene C_α and C_γ carbons are electrophilic while the C_β carbon is nucleophilic.^{11,13b} Likewise, it is well-known that phosphines such as PMe_3 ,^{21a,b} PPh_3 ,^{21c} and PET_3 ^{21c} will add to allenylidenes at C_γ ,^{11,12,21} however, the use of DPVP for this purpose has no precedent. Allenylidenes are also known to undergo C–C coupling reactions,^{21a,22} sometimes to form carbocycles,^{22b,c} but to the best of our knowledge the reaction between an olefinic phosphine and an allenylidene to form a heterocyclic vinylidene is unprecedented. In contrast to the reaction of **6** with a phosphine, the closely related ruthenium analog, $[(\eta^5\text{-C}_5\text{Me}_5)(\text{PPhMe}_2)_2\text{Ru}\{\text{C}=\text{C}(\text{H})(\text{CH}_2\text{OH})\}][\text{PF}_6]$, reportedly did *not* react with PPh_3 via an allenylidene intermediate to form the corresponding phosphonium salt.¹⁰

The $^{31}\text{P}\{^1\text{H}\}$ NMR spectrum of **7** in acetonitrile- d_3 shows a broad singlet at 35.7 ppm and a sharp singlet at 42.9 ppm in a 2:1 ratio corresponding to the two η^1 -DPVP ligands and the phosphonium phosphorus, respectively. The ^1H NMR data in nitromethane- d_3

Table 5. Selected Bond Distances and Angles for $[(\eta^5\text{-C}_5\text{Me}_5)\text{Ru}(\eta^1\text{-DPVP})_2\{\text{C}=\text{C}(\text{CH}_2)_2\text{PPh}_2\text{CH}_2\}][\text{PF}_6]_2$ (7**)**

Bond Distances (Å)			
Ru1–P1	2.345(3)	P3–C44	1.788(13)
Ru1–P2	2.357(3)	P3–C50	1.807(13)
Ru1–C39	1.816(12)	C11–C12	1.275(14)
C39–C40	1.33(2)	C25–C26	1.32(2)
C40–C41	1.54(2)	Ru1–C1	2.279(12)
C41–C42	1.522(14)	Ru1–C2	2.273(13)
P3–C42	1.782(12)	Ru1–C3	2.334(12)
P3–C43	1.831(11)	Ru1–C4	2.328(11)
C40–C43	1.53(2)	Ru1–C5	2.283(12)
		Ru1–Cp ^a	1.957

Bond Angles (deg)			
P1–Ru1–P2	93.47(13)	C42–P3–C43	95.5(5)
C39–Ru1–P1	88.2(4)	C43–C40–C41	113.6(11)
C39–Ru1–P2	92.4(4)	C42–P3–C44	111.3(6)
C401–C39–Ru1	175.5(11)	C42–P3–C50	110.0(6)
C39–C40–C41	122.2(13)	C44–P3–C43	109.5(6)
C39–C40–C43	124.2(12)	C44–P3–C50	112.2(6)
C42–C41–C40	110.1(11)	C50–P3–C43	116.3(6)
C41–C42–P3	104.7(8)		

^a Cp^{*} denotes the centroid of the C(1–5) ring.

show three methylene resonances at 4.40, 3.83, and 3.27 ppm. The downfield resonance at 4.40 ppm appears as a doublet ($^2J_{\text{PH}} = 11.0$ Hz) corresponding to the CH_2 group bound directly to the vinylidene $\text{Ru}=\text{C}=\text{C}_\beta$ carbon and the phosphonium phosphorus. The resonance at 3.83 ppm appears as a doublet of triplets ($^3J_{\text{PH}} = 15.0$ Hz, $^3J_{\text{HH}} = 7.5$ Hz) and represents the other CH_2 group bound to the $\text{Ru}=\text{C}=\text{C}_\beta$ carbon. Finally, the remaining CH_2 group appears at 3.27 ppm as a doublet of triplets ($^2J_{\text{PH}} = 10.5$ Hz, $^3J_{\text{HH}} = 7.5$ Hz). The $^{13}\text{C}\{^1\text{H}\}$ NMR spectrum shows the $\text{Ru}=\text{C}_\alpha$ carbon resonance as a triplet at 341.1 ppm ($^2J_{\text{PC}} = 13.8$ Hz) while the resonances for the three CH_2 carbons of the trihydrophosphonium ring appear as doublets at 24.8 ($^1J_{\text{PC}} = 4.1$ Hz), 24.3 ($^2J_{\text{PC}} = 1.7$ Hz) and 23.3 ppm ($^1J_{\text{PC}} = 2.1$ Hz), respectively.

A view of the geometry of the cation of **7** is shown in Figure 4. Selected bond distances and angles are listed in Table 5. The analysis reveals a distorted octahedral geometry at ruthenium with one facial $\eta^5\text{-C}_5\text{Me}_5$ moiety, two η^1 -DPVP ligands, and the vinylidene phosphonium moiety completing the coordination sphere. The interligand bond angles of 93.47(13)° for P1–Ru1–P2, 88.2(4)° for C39–Ru1–P1, and 92.4(4)° for C39–Ru1–P2 reflect the distorted octahedral geometry at ruthenium. The Ru1–C39 bond length in **7** is 1.816(12) Å and the C39–C40 bond distance is 1.33(2) Å, which are typical vinylidene bond lengths.¹¹ The C40–C41 and C40–C43 bond lengths are 1.54(2) and 1.53(2) Å, respectively, and are typical^{23 a–c} for alkylvinylidene ($=\text{C}_\beta\text{–C}$) bond lengths, which range from 1.485(11) Å^{23c} for $[(\eta^5\text{-C}_5\text{H}_5)\text{Ru}(\text{PMe}_3)_2\{\text{C}=\text{C}(\text{H})(\text{CH}_3)\}][\text{PF}_6]$ to 1.55 Å^{23a} for $[(\eta^5\text{-C}_5\text{H}_5)(\text{Ph}_2\text{P}(\text{CH}_2)_2\text{PPh}_2)\text{Ru}\{\text{C}=\text{C}(\text{Ph})(\text{C}_7\text{H}_7)\}][\text{PF}_6]$. The P3–C43 and P3–C42 bond lengths in **7** are 1.831(11) and 1.782(12) Å, respectively, which are typical phosphorus–carbon bond distances. Analysis of the bond angles at P3 indicate that the coordination geometry is that of a distorted tetrahedron (see Table 5). The trihydrophosphonium ring adopts an envelope confor-

(22) (a) Wiedemann, R.; Steinert, P.; Gevert, O.; Werner, H. *J. Am. Chem. Soc.* **1996**, *118*, 2495. (b) Bruce, M. I.; Hinterding, P.; Tiekink, E. R. T.; Skelton, B. W.; White, A. H. *J. Organomet. Chem.* **1993**, *450*, 209. (c) Selegue, J. P. *J. Am. Chem. Soc.* **1983**, *105*, 5921. (d) Antonova, A. B.; Loganov, A. A. *Russ. Chem. Rev.* **1989**, *58*, 693. (e) Braun, T.; Meuer, P.; Werner, H. *Organometallics* **1996**, *15*, 4075.

(23) (a) Bruce, M. I.; Dean, C.; Duffy, D. N.; Humphrey, M. G.; Koutsantonis, G. A. *J. Organomet. Chem.* **1985**, *295*, C40. (b) Bruce, M. I.; Humphrey, M. G.; Snow, M. R.; Tiekink, E. R. T. *J. Organomet. Chem.* **1986**, *314*, 213. (c) Bruce, M. I.; Wong, F. S.; Skelton, B. W.; White, A. H. *J. Chem. Soc., Dalton Trans.* **1982**, 2203.

mation and the deviations from the mean plane defined by C39, C40, C41, and C43 are as follows: C39 -0.0016 Å, C40 0.0042 Å, C41 -0.0013 Å, C42 -0.1201 Å, P3 -0.8452 Å, and C43 -0.0013 Å. The vinylidene is nearly linear with a Ru1–C39–C40 bond angle of 175.5 – $(11)^\circ$. In **7**, the vinylidene plane defined by Ru1–C39–C40–C41 makes an angle of 82.1° with the plane bisecting the P1–Ru–P2 angle, as expected.^{11,12} The formation of **7** suggests that primary allenylidenes can be used in the synthesis of novel heterocycles.

Summary

The synthesis, characterization, and properties of the phosphaallyl **1** are presented for the first time. Compound **1** contains the bidentate, olefinic phosphine η^3 -DPVP ligand, which displays hemilabile properties as illustrated by displacement of the olefin with CO and terminal acetylenes. Compound **7** represents a novel cyclization product between an olefinic phosphine and a primary allenylidene. Compound **1** may be useful as a catalyst for carbon–carbon bond formation involving the coupling of terminal acetylenes with alkenes. Studies in this area are currently in progress.

Experimental Section

A. Reagents and Physical Measurements. All chemicals were reagent grade and were used as received from commercial sources (Aldrich or Fisher Scientific) or synthesized as described below. Diphenylvinylphosphine was purchased from Organometallics. HPF_6 (60 wt % solution in water) was purchased from Aldrich and used as received. Solvents were dried by standard procedures and stored over Linde type 4Å molecular sieves. All syntheses were conducted in Schlenk glassware under a nitrogen atmosphere. $\text{HC}_5\text{Me}_5^{24}$ and $[(\eta^5\text{-C}_5\text{Me}_5)\text{RuCl}_2]_2^{27}$ were synthesized by literature procedures. Elemental analyses were performed by Galbraith Laboratories, Knoxville, TN. Melting points were obtained using a Mel-Temp melting point apparatus and are uncorrected. ^1H , $^1\text{H}\{^3\text{P}\}$, and $^{13}\text{C}\{^1\text{H}\}$ NMR spectra were recorded at 499.8, 499.8, and 125.7 MHz, respectively, on a Varian Unity Plus 500 FT-NMR spectrometer. Proton and carbon chemical shifts are relative to internal Me_4Si or solvent resonances. $^{31}\text{P}\{^1\text{H}\}$ NMR spectra were recorded at 121.65 MHz on a General Electric GN 300 FT-NMR spectrometer. Phosphorus chemical shifts are relative to external 85% $\text{H}_3\text{PO}_4(\text{aq})$ with positive values being downfield of the respective reference. Unless otherwise stated, all chromatography was performed using the following general procedure: A 60 mL sintered glass fritted funnel was used as the column and attached to a 1000 mL Erlenmeyer flask equipped with a side arm. A 2.5 cm layer of silica gel (grade 12, 28–300 mesh, Aldrich) was covered with Celite (Aldrich, 0.5 cm layer) and firmly packed with a spatula and suction. The crude reaction product was dissolved in a minimal amount of a volatile solvent (usually CH_2Cl_2) and loaded onto the column, and the solvent was removed with suction. All subsequent solvents were eluted with suction.

B. Syntheses. Preparation of $[(\eta^5\text{-C}_5\text{Me}_5)\text{Ru}(\eta^3\text{-DPVP})(\eta^1\text{-DPVP})]\text{PF}_6$ (1**).** A 250 mL, three-neck round-bottom flask was fitted with a septum, gas inlet adapter, and a U-tube adapter. A glass frit funnel was attached to both the U-tube and a second 250 mL round-bottom flask equipped with two necks. The entire apparatus was flame-dried under vacuum and flushed with nitrogen. The first flask was charged with $[(\eta^5\text{-C}_5\text{Me}_5)\text{RuCl}_2]_2$ (2.5 g, 4.1 mmol), powdered zinc (6.6 g, 101

mmol), and 100 mL of freshly distilled CH_3CN . The dark red mixture was stirred vigorously for 2 h and gradually turned from red to green to yellow/brown. The excess zinc was removed by filtration under nitrogen and washed with 2×5 mL portions of CH_3CN . The yellow/brown filtrate was charged with diphenylvinylphosphine (3.64 mL, 18.3 mmol), and the solution was stirred at room temperature for 8 h. To this mixture was added a solution of NaPF_6 (1.7 g, 10.1 mmol) in 35 mL of MeOH. A precipitate formed upon addition of the salt solution. The reaction mixture was stirred for 45 min, after which all solvents were removed *in vacuo*. The resulting brown residue was dissolved in a minimal amount of CH_2Cl_2 and filtered, and the solvent was removed *in vacuo*. The yellow/brown residue was flash chromatographed over Celite/silica gel with 1250 mL of CH_2Cl_2 to give a yellow solution. The solvent was removed *in vacuo*, and the yellow amorphous solid was dried under high vacuum for 24 h to give 4.7 g of **1** in 72% yield. The product was recrystallized from boiling absolute EtOH before use in subsequent reactions. Mp: 190–191 $^\circ\text{C}$. Anal. Calcd for $\text{C}_{38}\text{H}_{41}\text{F}_6\text{P}_3\text{Ru}$: C, 56.65; H, 5.13. Found: C, 56.59; H, 5.02. ^1H NMR (CDCl_3): δ 6.9–7.9 (m, 20H, Ph), 5.35 (ddd, $^3J(\text{PH}_b) = 36.06$ Hz, $^3J(\text{H}_a\text{H}_b) = 12.32$ Hz, $^2J(\text{H}_b\text{H}_c) = 0.6$ Hz, 1H, H_b), 5.03 (ddd, $^3J(\text{PH}_c) = ^3J(\text{H}_a\text{H}_c) = 17.43$ Hz, $^2J(\text{H}_b\text{H}_c) = 0.6$ Hz, 1H, H_c), 4.25 (ddd, $^2J(\text{PH}_a) = 26.15$ Hz, $^3J(\text{H}_a\text{H}_c) = 17.43$ Hz, $^3J(\text{H}_a\text{H}_b) = 12.32$ Hz, 1H, H_a), 3.20 (m, $^3J(\text{PH}_b) = 34.86$ Hz, $^3J(\text{PH}_b) = 1.80$ Hz, $^3J(\text{H}_a\text{H}_b) = 10.37$ Hz, $^2J(\text{H}_b\text{H}_c) = 9.91$ Hz, 1H, H_b), 3.12 (m, $^2J(\text{PH}_a) = 13.22$ Hz, $^3J(\text{PH}_a) = 2.10$ Hz, $^3J(\text{H}_a\text{H}_b) = 10.37$ Hz, $^3J(\text{H}_a\text{H}_c) = 0.62$ Hz, 1H, H_a), 2.62 (m, $^3J(\text{PH}_c) = 16.23$ Hz, $^3J(\text{PH}_c) = 6.31$ Hz, $^2J(\text{H}_b\text{H}_c) = 9.91$ Hz, $^3J(\text{H}_a\text{H}_c) = 0.62$ Hz, 1H, H_c), 1.29 (apparent t, $^4J(\text{PH}) = ^4J(\text{P'H}) = 1.5$ Hz, 15H, CH_3). $^{13}\text{C}\{^1\text{H}\}$ NMR (CDCl_3): δ 136.20 (d, $^2J(\text{PC}) = 12.47$ Hz, C_o), 133.17 (d, $^2J(\text{PC}) = 9.82$ Hz, C_o), 132.06 (d, $^2J(\text{PC}) = 10.66$ Hz, C_o), 132.01 (d, $^2J(\text{PC}) = 12.09$ Hz, C_o), 131.63 (d, $^1J(\text{PC}) = 45.85$ Hz, C_o), 131.28 (s, C_p), 103.54 (s, C_p), 129.75 (d, $^3J(\text{PC}) = 11.56$ Hz, C_m), 129.53 (d, $^3J(\text{PC}) = 11.56$ Hz, C_m), 129.48 (dd, $^1J(\text{PC}) = 68.40$ Hz, $^3J(\text{PC}) = 4.08$ Hz, C_i), 129.02 (d, $^2J(\text{PC}) = 4.9$ Hz, C_p), 128.60 (d, $^3J(\text{PC}) = 9.22$ Hz, C_m), 128.50 (d, $^3J(\text{PC}) = 10.05$ Hz, C_m), 128.44 (d, $^1J(\text{PC}) = 54.57$ Hz, C_i), 127.75 (dd, $^1J(\text{PC}) = 43.99$ Hz, $^3J(\text{PC}) = 4.75$ Hz, C_i), 96.45 (s, C_5Me_5), 47.87 (d, $^2J(\text{PC}) = 7.2$ Hz, C_p), 37.55 (d, $^1J(\text{PC}) = 33.8$ Hz, C_a), 9.01 (t, $^3J(\text{PC}) = ^3J(\text{P'C}) = 11.2$ Hz, CH_3). $^{31}\text{P}\{^1\text{H}\}$ NMR (CDCl_3): δ 44.85 (d, $^2J(\text{PP}) = 48.5$ Hz, $\eta^1\text{-DPVP}$), 14.29 (d, $^2J(\text{PP}) = 48.5$ Hz, $\eta^3\text{-DPVP}$), -144.1 (septet, $^1J(\text{PF}) = 712.8$ Hz, PF_6^-).

Preparation of $[(\eta^5\text{-C}_5\text{Me}_5)\text{Ru}(\eta^1\text{-DPVP})_2(\text{NCS})]$ (2**).** A 25 mL Schlenk flask was charged with **1** (0.15 g, 0.19 mmol), 10 mL of CH_2Cl_2 , and a solution of NaNCS (0.13 g, 1.6 mmol) in 10 mL of MeOH. The solution was stirred vigorously for 20 h and gradually turned from yellow to red. The solvents were removed *in vacuo*, and the residue was dissolved in a minimal amount of CH_2Cl_2 and filtered. The filtrate was evaporated, and the product was extracted with 4×20 mL of Et_2O . The Et_2O washings were combined, evaporated to dryness, and dried to give 0.09 g of **2** in 67% yield. The product is mildly air sensitive in solution. Mp: 225 $^\circ\text{C}$ dec. Anal. Calcd for $\text{C}_{38}\text{H}_{41}\text{NP}_2\text{RuS}$: C, 65.16; H, 5.57. Found: C, 65.02; H, 5.38. ^1H NMR (CDCl_3): δ 7.56–6.96 (m, 20 H, Ph), 5.69 (m, 4H, $\text{H}_{a,b}$), 5.19 (m, 2H, H_c), 1.33 (t, $^4J(\text{PH}) = 1.5$ Hz, 15H, CH_3). $^{13}\text{C}\{^1\text{H}\}$ NMR (CDCl_3): δ 136.56 (D, $^1J(\text{PC}) + ^3J(\text{PC}) = 41.4$ Hz, C_i), 134.84 (T, $^2J(\text{PC}) + ^4J(\text{PC}) = 11.8$ Hz, C_o), 133.78 (D, $^1J(\text{PC}) + ^3J(\text{PC}) = 36.6$ Hz, C_o), 133.51 (D, $^1J(\text{PC}) + ^3J(\text{PC}) = 42.5$ Hz, C_i), 132.99 (T, $^2J(\text{PC}) + ^4J(\text{PC}) = 9.7$ Hz, C_o), 131.80 (D, $^2J(\text{PC}) + ^4J(\text{PC}) = 2.8$ Hz, C_p), 129.85 (s, C_p), 128.85 (s, C_p), 127.68 (T, $^3J(\text{PC}) + ^5J(\text{PC}) = 9.6$ Hz, C_m), 127.48 (T, $^3J(\text{PC}) + ^5J(\text{PC}) = 9.1$ Hz, C_m), 127.2 (t, $^3J(\text{PC}) = 1.9$ Hz, NCS), 90.16 (t, $^2J(\text{PC}) = 2.1$ Hz, C_5Me_5), 9.53 (s, CH_3). $^{31}\text{P}\{^1\text{H}\}$ NMR (CDCl_3): δ 39.0 (s).

Preparation of $[(\eta^5\text{-C}_5\text{Me}_5)\text{Ru}(\eta^1\text{-DPVP})_2(\text{CO})]\text{PF}_6$ (3**).** A 50 mL flask was charged with **1** (0.15 g, 0.19 mmol) and 20 mL of 1,2-dichloroethane. A Tygon tube, fitted to a gas inlet adapter, was inserted into the solution. This solution was then heated to reflux under a CO atmosphere for 116 h. The solvent

(24) Fendrick, C. M.; Schertz, L. D.; Mintz, E. A.; Marks, T. J. *Inorg. Synth.* **1992**, 29, 193.

Table 6. Crystallographic Data for 1, 4, 5, and 7

	1	4	5	7
empirical formula	C ₃₈ H ₄₁ F ₆ P ₃ Ru	C ₄₆ H ₄₇ F ₆ P ₃ Ru	C ₄₂ H ₄₇ F ₆ OP ₃ Ru	C ₅₅ H ₅₇ F ₁₂ P ₅ Ru
fw	805.7	907.82	875.78	1201.93
cryst dimens (mm)	0.15 × 0.30 × 0.40	0.18 × 0.2 × 0.3	0.46 × 0.25 × 0.84	0.10 × 0.17 × 0.42
cryst syst	orthorhombic	orthorhombic	triclinic	monoclinic
space group	<i>Pca</i> 2 ₁	<i>Pbca</i>	<i>P</i> $\bar{1}$	<i>P</i> 2 ₁ / <i>c</i>
<i>a</i> (Å)	17.291(5)	15.275(2)	13.119(2)	10.359(2)
<i>b</i> (Å)	14.313(4)	22.723(3)	15.605(2)	27.270(5)
<i>c</i> (Å)	29.640(8)	24.834(2)	20.538(3)	19.081(3)
α (deg)	90	90	106.424(11)	90
β (Å)	90	90	93.550(12)	90.606(14)
γ (Å)	90	90	90.923(12)	90
<i>V</i> (Å ³)	7335(6)	8620(2)	4022.8(10)	5390(2)
<i>Z</i>	8	8	4	4
<i>d</i> _{calcd} (g/cm ³)	1.459	1.399	1.446	1.481
μ (mm ⁻¹)	0.6027	0.532	0.569	0.518
radiation (λ = 0.710 73 Å)	Mo K α	Mo K α	Mo K α	Mo K α
temp (K)	293	298	298	298
scan type	$\omega/2\theta$	ω	ω	ω
2 θ range (deg)	4–50	3.58–45	3.62–45	3.68–45
no. of reflns collcd	7093	6845	12 080	8870
no. of indepnt reflns	7093	5637 (<i>R</i> _{int} = 0.1018)	10415 (<i>R</i> _{int} = 0.0187)	7049 (<i>R</i> _{int} = 0.0934)
abs corr	ψ -scans	ψ -scans	ψ -scans	ψ -scans
max and min transmission	1 and 0.95	0.7447 and 0.7317	0.9742 and 0.7831	0.7723 and 0.7158
data/restraints/params	3822/1/864	5635/0/505	10415/0/1001	7046/0/695
<i>R</i> ₁ , <i>wR</i> ₂ ^c [<i>I</i> > 2 σ (<i>I</i>)]	0.040, 0.052 ^a	0.082, 0.1087	0.0409, 0.0947	0.0849, 0.1029
goodness of fit (<i>F</i> ²) ^d	1.079	0.989	1.308	1.014
extinction coeff	0	0	0.00040(11)	0
largest diff peak and hole (e Å ⁻³)	0.87/–0.58	0.38/–0.41	0.54/–0.46	0.44/–0.40

^a [*I* > 3 σ (*I*)]. ^b *R*₁(*F*) = $\sum||F_o| - |F_c||/\sum|F_o|$. ^c *wR*₂(*F*²) = $[\sum[w(F_o^2 - F_c^2)^2]/\sum[w(F_o^2)^2]]^{0.5}$. ^d GOF = *S* = $[\sum[w(F_o^2 - F_c^2)^2]/(n - p)]^{0.5}$.

was removed *in vacuo*, and the yellow residue was treated with 3 × 5 mL portions of Et₂O. The product was dried in high vacuum (0.1 mmHg) at 68 °C for 24 h to give 0.15 g of **3** in 94% yield. Mp: 182–183 °C. Anal. Calcd for C₃₈H₄₁F₆OP₃Ru: C, 56.18; H, 4.96. Found: C, 56.08; H, 5.04. ¹H NMR (CDCl₃): δ 6.76–7.76 (m, 20H, Ph), 5.93 (m, 2H, H_b), 5.45 (br m, 2H, H_a), 5.29 (m, 2H, H_c), 1.59 (t, ⁴J(PH) = 1.7 Hz, 15H, CH₃). ¹³C{¹H} NMR (CDCl₃): δ 204.25 (t, ²J(PC) = 17.2 Hz, CO), 134.23 (T, ²J(PC) + ⁴J(PC)) = 11.9 Hz, C_o), 132.33 (D, ¹J(PC) + ³J(PC)) = 47.0 Hz, C_a), 132.31 (T, ²J(PC) + ⁴J(PC)) = 9.7 Hz, C_o), 130.86 (D, ²J(PC) + ⁴J(PC)) = 5.7 Hz, C_β), 130.84 (s, C_p), 130.62 (s, C_p), 129.59 (D, ¹J(PC) + ³J(PC)) = 43.9 Hz, C_i), 128.96 (D, ¹J(PC) + ³J(PC)) = 50.9 Hz, C_i), 128.91 (T, ³J(PC) + ⁵J(PC)) = 10.6 Hz, C_m), 128.52 (T, ³J(PC) + ⁵J(PC)) = 10.1 Hz, C_m), 100.1 (t, ²J(PC) = 1.4 Hz, C₅Me₃), 9.72 (s, CH₃). ³¹P{¹H} NMR (CDCl₃): δ 35.3 (s), –144.1 (septet, ¹J(PF) = 712.8 Hz, PF₆[–]).

Preparation of [(η^5 -C₅Me₅)Ru(η^1 -DPVP)₂{C=C(H)(Ph)}]PF₆ (4**).** A 25 mL Schlenk flask was charged with **1** (0.20 g, 0.25 mmol), 20 mL of MeOH, and HC≡CPh (0.04 mL, 0.36 mmol). The solution was refluxed under N₂ for 16 h and rapidly turned from yellow to red. The reaction solution was then cooled to –25 °C for 48 h, from which an orange solid precipitated. The precipitate was collected on a glass frit, washed with 3 × 5 mL portions of Et₂O, and dried to give 0.12 g of **4** in 53% yield. Compound **4** can be recrystallized from hot methanol. Mp: 174–176 °C. Anal. Calcd for C₄₆H₄₇F₆P₃Ru: C, 60.86; H, 5.22. Found: C, 60.73; H, 5.09. ¹H NMR (CDCl₃): δ 6.68–7.64 (m, 25H, Ph), 5.79 (m, 2H, H_b), 5.65 (br m, 2H, H_a), 5.26 (t, ⁴J(PH) = 2.2 Hz, 1H, =C=CH), 5.01 (m, 2H, H_c), 1.62 (t, ⁴J(PH) = 1.5 Hz, 15H, CH₃). ¹³C{¹H} NMR (CDCl₃): δ 353.6 (m, Ru=C_a=), 134.4–126.99 (m, PC=C, Ph), 115.41 (s, Ru=C=C_β), 103.83 (br s, C₅Me₃), 9.96 (s, CH₃). ³¹P{¹H} NMR (CDCl₃): δ 38.0 (s), –144.2 (septet, ¹J(PF) = 712.7 Hz, PF₆[–]).

Preparation of (5) [(η^5 -C₅Me₅)Ru(η^1 -DPVP)₂{C(CH₂)₃O}]PF₆ (5**).** A 50 mL Schlenk flask was charged with **1** (0.20 g, 0.25 mmol), 20 mL of CH₂Cl₂, and HC≡CCH₂CH₂OH (0.04 mL, 0.53 mmol). The solution was stirred at room temperature for 15 h. The ³¹P{¹H} NMR spectrum of this solution contains a singlet at 38.0 ppm for the vinylidene adduct. This solution

was refluxed for 28 h. The mixture was then concentrated to a volume of about 10 mL, Et₂O (15 mL) was layered on top of the CH₂Cl₂ solution, and the mixture was stored at –25 °C for 48 h. The resulting yellow crystals were collected on a glass frit, washed with 3 × 5 mL portions of Et₂O, and dried to give 0.14 g of **5** in 63% yield. Anal. Calcd for C₄₂H₄₇F₆OP₃Ru: C, 57.60; H, 5.41. Found: C, 57.54; H, 5.32. ¹H NMR (CDCl₃):

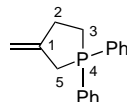


δ 6.61–7.59 (m, 20H, Ph), 5.67 (br m, 4H, H_{b,c}), 4.93 (br m, 2H, H_a), 4.31 (t, ³J(HH) = 7.0 Hz, 2H, C(3)H), 3.35 (t, ³J(HH) = 7.0 Hz, 2H, C(5)H), 2.11 (br m, 2H, C(4)H), 1.48 (br m, 15H, CH₃). ¹³C{¹H} NMR (CDCl₃): δ 299.50 (m, Ru=C_a=), 135.23 (br m), 133.78 (br), 133.11 (br), 131.37 (s), 130.01 (br), 128.27 (T, ³J(PC) + ⁵J(PC)) = 10.0 Hz, C_m), 127.08 (br), 126.64 (br), 99.32 (br, C₅Me₃), 80.86 (s, C3), 55.81 (s, C5), 23.41 (s, C4), 10.04 (s, CH₃). ³¹P{¹H} NMR (CDCl₃): δ 45.1 (s), –144.4 (septet, ¹J(PF) = 712.8 Hz).

Preparation of [(η^5 -C₅Me₅)Ru(η^1 -DPVP)₂{C=C(H)-CH₂OH}]PF₆ (6**).** A 25 mL Schlenk flask was charged with **1** (0.25 g, 0.31 mmol), 12 mL of CHCl₃, and HC≡CCH₂OH (0.035 mL, 0.60 mmol). The solution was stirred at room temperature for 72 h and a yellow solid gradually precipitated out of solution. The yellow precipitate was isolated on a glass frit, washed with 2 × 5 mL portions of hexanes, and dried to give 0.16 g of **6** in 60% yield. Anal. Calcd for C₄₁H₄₅F₆OP₃Ru: C, 57.14; H, 5.26. Found: C, 57.07; H, 5.14. ¹H NMR {(CD₃)₂C=O}: δ 7.78–6.78 (m, 20H, Ph), 5.95 (m, 2H, H_b), 5.79 (br m, 2H, H_c), 5.17 (m, 2H, H_a), 4.88 (tt, ³J(HH) = 8.0 Hz, ⁴J(PH) = 2.2 Hz, 1H, =C=CH), 4.49 (dd, ³J(HH) = 8.0 Hz, ³J(HH) = 5.8 Hz, 2H, CH₂), 4.19 (t, ³J(HH) = 5.8 Hz, 1H, OH), 1.63 (t, ⁴J(PH) = 1.5 Hz, 15H, CH₃). ¹³C{¹H} NMR {(CD₃)₂C=O}: δ 351.00 (t, ²J(PC) = 15.7 Hz, Ru=C_a=), 135.69 (T, ²J(PC) + ⁴J(PC)) = 11.8 Hz, C_o), 133.99 (T, ²J(PC) + ⁴J(PC)) = 9.7 Hz, C_o), 132.90 (s, C_β), 131.75 (s, C_β), 131.60 (m, C_i), 131.24 (m, C_i), 130.77 (D, ¹J(PC) + ³J(PC)) = 51.5 Hz, C_a, DPVP), 130.64 (s, C_β, DPVP), 129.72 (T, ³J(PC) + ⁵J(PC)) = 10.3 Hz, C_m), 129.29 (T, ³J(PC) + ⁵J(PC)) = 10.2 Hz, C_m),

112.08 (t, $^3J(\text{PC}) = 1.2$ Hz, $\text{Ru}=\text{C}=\text{C}_\beta$), 104.06 (t, $^2J(\text{PC}) = 1.4$ Hz, C_5Me_5), 53.93 (s, CH_2), 10.04 (s, CH_3). $^{31}\text{P}\{^1\text{H}\}$ NMR ($\text{CH}_2\text{-Cl}_2$): δ 39.3 (s), -144.4 (septet, $^1J(\text{PF}) = 712.8$ Hz, PF_6^-).

Preparation of $[(\eta^5\text{-C}_5\text{Me}_5)\text{Ru}(\eta^1\text{-DPVP})_2\{\text{C}=\text{C}(\text{CH}_2)_2\text{PPh}_2\text{CH}_2\}][\text{PF}_6]_2$ (7**).** A 50 mL Schlenk flask was charged with **6** (0.20 g, 0.17 mmol) and 20 mL of CH_3CN . The reaction solution was stirred at room temperature under N_2 until the color of the solution changed from yellow/orange to violet (~24 h). The reaction mixture was then charged with DPVP (0.04 mL, 0.20 mmol) and HPF_6 (0.03 mL, 0.20 mmol) and refluxed for 24 h. The solution volume was then reduced to 10 mL, and 20 mL of Et_2O was added. The rose/pink precipitate was collected on a glass frit and washed with 3×10 mL portions of Et_2O . The product was recrystallized from $\text{CH}_2\text{Cl}_2/\text{Et}_2\text{O}$ to give 0.09 g of **7** in 44% yield. Anal. Calcd for $\text{C}_{55}\text{H}_{57}\text{F}_{12}\text{P}_5\text{Ru}$: C, 54.96; H, 4.78. Found: C, 54.79; H, 4.68. ^1H NMR ($\text{CD}_3\text{-}$



NO_2): δ 7.98–6.72 (m, 30H, Ph), 5.88 (br, 4H, $\text{H}_{b,c}$), 5.16 (br, 2H, H_a), 4.40 (d, $^2J(\text{PH}) = 11.0$ Hz, 2H, $\text{C}(5)\text{H}_2$), 3.83 (dt, $^3J(\text{PH}) = 15.0$ Hz, $^3J(\text{HH}) = 7.5$ Hz, 2H, $\text{C}(2)\text{H}_2$), 3.27 (dt, $^2J(\text{PH}) = 10.5$ Hz, $^3J(\text{HH}) = 7.5$ Hz, 2H, $\text{C}(3)\text{H}_2$), 1.57 (t, $^4J(\text{PH}) = 0.9$ Hz, 15H, CH_3). $^{13}\text{C}\{^1\text{H}\}$ NMR (CD_3NO_2): δ 341.1 (br, $\text{Ru}=\text{C}_\alpha$), 137.1 (s, C_p , Ph_2P^+), 136.3 (br, C_o , DPVP), 134.5 (br, C_m , DPVP), 134.22, (d, $^2J(\text{PC}) = 10.8$ Hz, C_o , Ph_2P^+), 133.63 (s, C_p , Ph_2P^+), 133.13 (s, C_p , DPVP), 132.4 (s, C_o , DPVP), 131.88 (d, $^2J(\text{PC}) = 12.7$ Hz, C_o , Ph_2P^+), 131.1 (br, C_i , DPVP), 130.7 (br, C_i , DPVP), 130.16 (d, $^3J(\text{PC}) = 10.1$ Hz, C_m , Ph_2P^+), 129.88 (d, $^3J(\text{PC}) = 10.2$ Hz, C_m , Ph_2P^+), 118.98 (d, $^1J(\text{PC}) = 81.3$ Hz, C_i , Ph_2P^+), 116.12 (d, $^2J(\text{PC}) = 9.8$ Hz, $\text{Ru}=\text{C}=\text{C}_\beta$), 106.19 (t, $^2J(\text{PC}) = 1.3$ Hz, C_5Me_5), 24.80 (d, $^1J(\text{PC}) = 4.1$ Hz, C_5), 24.37 (d, $^2J(\text{PC}) = 1.7$ Hz, C_2), 23.28 (d, $^1J(\text{PC}) = 2.1$ Hz, C_3), 10.41 (s, CH_3). $^{31}\text{P}\{^1\text{H}\}$ NMR (CD_3CN): δ 42.9 (s, 1P, Ph_2P^+), 35.7 (br s, 2P, DPVP), -145.2 (septet, $^1J(\text{PF}) = 712.8$ Hz, PF_6^-).

C. X-ray Determination and Processing for **1, **4**, **5**, and **7**.** Crystal data and details of data collection for **1**, **4**, **5**, and **7** are given in Table 6. Data for **1** were collected in the $\omega/2\theta$ mode while data for **4**, **5**, and **7** were collected in the ω mode. All data were collected with Mo $\text{K}\alpha$ graphite-monochromated radiation ($\lambda = 0.71073$ Å). Yellow crystals of **1** were grown from boiling absolute ethanol. Data were collected using an Enraf-Nonius CAD4-F automatic diffractometer at room temperature. Three standard reflections measured every hour during the entire data collection period showed no significant trend. The raw data were converted to intensities and corrected for Lorentz, polarization, and absorption factors. The structure was solved by the heavy atom method. After refinement of the non-hydrogen atoms, difference Fourier maps revealed maximums of residual electron density close to positions expected for hydrogen atoms. Hydrogen atoms

were refined at calculated positions with a riding model in which the C–H vector was fixed at 0.95 Å with isotropic temperature factors such as $B(\text{H}) = 1.3$ Beqv ($^\circ\text{C}$) Å. A final Fourier difference map revealed no significant maximums. All calculations were performed on a VAX computer using the Enraf-Nonius VAX/Molen package.²⁵ The absolute structure was determined by comparing R , R_w , and GOF for x , y , z and $-x$, $-y$, $-z$ refinements and confirmed by refinement of Flack's $x = 0.20(2)$.²⁶ Neutral atom scattering factor coefficients and anomalous dispersion coefficients were taken from a standard source.²⁷

Orange crystals of **4** were grown from boiling methanol; yellow crystals of **5** and pink/orange crystals of **7** were grown by slow diffusion of Et_2O into saturated CH_2Cl_2 solutions. The crystals were coated with epoxy, mounted on glass fibers, and placed on a Siemens P4 diffractometer. Two check reflections, monitored every 100 reflections, showed random (<2%) variation during the data collection. Unit cell parameters were determined by least-squares refinement of 24 reflections for **4**, **5**, and **7**. The data were corrected for Lorentz, polarization, and absorption (using an empirical model derived from azimuthal data collections). Scattering factors and corrections for anomalous dispersion were taken from a standard source.²⁸ Calculations were performed with the Siemens SHELXTL Plus version 5.1 software package on a personal computer. The structures were solved by direct methods. Anisotropic thermal parameters were assigned to all non-hydrogen atoms. Hydrogen atoms were refined at calculated positions with a riding model in which the C–H vector was fixed at 0.96 Å. The PF_6^- ions of structures **5** and **7** are disordered.

Acknowledgment. We are grateful to the National Science Foundation (Grant CHE-9214294) for funds to purchase the Varian Unity Plus 500 MHz NMR spectrometer and to Johnson Matthey Aesar/Alfa for a generous loan of $\text{RuCl}_3 \cdot 3\text{H}_2\text{O}$. We thank Dr. Vincent J. Catalano for his training and assistance in determining the X-ray crystal structures of **4**, **5**, and **7**.

Supporting Information Available: For **1**, **4**, **5**, and **7**, listings of atomic coordinates and isotropic displacement parameters, H atom coordinates and isotropic displacement parameters, anisotropic displacement parameters— U values, and bond distances and angles (65 pages). Ordering information is given on any current masthead page.

OM961068J

(25) Molen, An Interactive Structure Solution Procedure, Enraf-Nonius, Delft, The Netherlands, 1990.

(26) Flack, H. D. *Acta Crystallogr.* **1983**, A39, 876.

(27) Cromer, D. T.; Waber, J. T. *International Tables for X-ray Crystallography*; The Kynoch Press: Birmingham, England, 1974; Vol. IV.

(28) *International Tables for X-Ray Crystallography*; D. Reidel Publishing Co.: Boston, 1992; Vol. C.